Metagenomic insight into shifts of methane-cycling communities following pasture conversion in the Amazon basin

Dasiel Obregon Alvarez (dasieloa@uoguelph.ca)
University of São Paulo
Leandro Fonseca de Souza
University of São Paulo
Lucas William Mendes
University of São Paulo
Moacir Tuzzin de Moraes
University of São Paulo
Micaela Tosi
University of Guelph
Andressa Monteiro Venturini
University of São Paulo
Kyle M. Meyer
University of California – Berkeley
Plínio Barbosa de Camargo
University of São Paulo
Brendan J.M. Bohannan
University of Oregon
Jorge L. Mazza Rodrigues
University of California – Davis
Kari E. Dunfield
University of Guelph
Siu Mui Tsai
University of São Paulo

Research Article

Keywords: land-use change, methanogens, methanotrophs, soil properties, multimodel inference

Posted Date: April 13th, 2022

DOI: https://doi.org/10.21203/rs.3.rs-1543615/v1

Abstract

Background: Deforestation threatens the integrity of the Amazon biome and the ecosystem services it provides. Most of this deforested land is converted to pastures for cattle raising. Early studies revealed that forest-to-pasture conversion alters the flux of methane gas (CH4) in Amazonian soils, driving a switch from acting as a sink to a source of atmospheric CH4. We sought to better understand this phenomenon by investigating the soil microbial metagenomes, focusing on the taxonomic and functional structure of methane-cycling communities. Results: Metagenomic data were combined with in situ measurements of CH4 fluxes, and measurements of soil edaphic factors. We found a significantly higher abundance of methanogens and reduced methanotrophs in pasture soils. As inferred by co-occurrence networks, these microorganisms seem to be less interconnected within the soil microbiota in pasture soils. Metabolic traits were also different between land uses, with increased hydrogenotrophic and methylotrophic pathways of methanogenesis in pasture soils. Similarly, methanotrophs harboring the soluble form of methane monooxygenase enzyme (sMMO) were depleted in pasture soils. Redundancy analysis and multimodel inference revealed that the shift in methane-cycling communities in pasture soils was associated with higher soil compaction, pH, organic matter, and micronutrients. Conclusions: These results provide new knowledge about the effect of forest-to-pasture conversion on the community traits of methane-cycling microorganisms in the Amazon region, resulting in increased abundance and functional potential of methanogens in pastures, and thus increasing the emission of CH4 in deforested soils. Keywords: land-use change, methanogens, methanotrophs, soil properties, multimodel inference

Background

The Amazon basin, with around 5.3 million km^2, constitutes 40% of the world's rainforests. This biome provides important local, regional, and global ecosystem services [1], including climate regulation, carbon sequestration, hydrologic cycling, and greenhouse gas (GHG) uptake [2, 3]. However, despite enormous efforts to preserve the Amazon biome over the last decades, deforestation and agribusiness continue to threaten this tropical forest [4–6]. It is estimated that ~ 20% of the Brazilian Amazon forest has already been converted into agricultural areas [5], with the predominant use being cattle ranching (~ 80%), followed by soybean cultivation [7]. Amazon deforestation and cattle ranching are closely intertwined with GHG emissions in Brazil [8, 9]. Methane (CH_4) is a powerful GHG and the second largest contributor to climate change after CO_2 [10]. Research over the last 20 years has revealed that Amazonian soils become sources of CH_4 to the atmosphere following conversion from forest to pasture [11, 12]. A recent study conducted by Meyer et al. [13] in two different Amazonian regions confirmed this trend in the CH_4 flux, recording high levels of CH_4 emission in pasture soils, and modest but variable levels of CH_4 uptake in primary forest soils.

CH_4 cycling in upland soils is mostly driven by methane producers (methanogens), which are strictly anaerobic archaea, and by methane-oxidizing bacteria (methanotrophs), which use CH_4 as a carbon and energy source. It is estimated that 50–90% of the CH_4 produced belowground is oxidized by

methanotrophs before reaching the atmosphere [14, 15]. This suggests that CH_4 cycling is more closely related to microbial community dynamics (i.e., more sensitive to microbial community disturbances) than any other biogeochemical processes [16]. Land-use change has been shown to lead to an increase in CH_4 fluxes or a decrease in the strength of upland soils as a CH_4 sink in other systems [17]. However, the underlying transformations of methanogens and methanotrophs communities in these contexts are not well understood [18–20].

Methanogenesis is the final step in the anaerobic degradation of organic matter [21, 22]. Depending on the available substrates, three main metabolic pathways are used: (i) hydrogenotrophic, (ii) acetoclastic, and (iii) methylotrophic methanogenesis [23]. Acetoclastic and hydrogenotrophic pathways are the most common methanogenic pathways and contribute around 67% and 33% of CH_4 biosynthesis, respectively [14, 15]. The role of methylotrophic methanogenesis is less clear [22]. However, the recent discovery of hydrogen-dependent methylotrophic methanogens in the order Methanomassiliicoccales suggests a higher ubiquitousness of these microbes than previously thought [24]. The last step of the three methanogenesis pathways consists of the reduction of methyl-coenzyme M to CH_4, which is catalyzed by the methyl-coenzyme M reductase (MCR) enzyme complex [23]. Two forms of MCR exist: The MCR-I which is present in all methanogens, while the isoenzyme MCR-II is only present in members of the class Methanococci and the Methanobacteria [25]. Concerning methanotrophy, the Type I methanotrophs (γ-Proteobacteria) use the ribulose monophosphate (RuMP) pathway, while type II (α-Proteobacteria) use the serine pathway [26]. The first step in both methanotrophy pathways consists of the oxidation of CH_4 to methanol (CH_3OH), catalyzed by the enzyme methane monooxygenase (MMO) [26, 27]. Two forms of MMO have been identified, the most common is a copper-containing membrane-bound enzyme particulate MMO (pMMO) found in nearly all methanotrophs, while the cytosolic iron-containing soluble (sMMO) form is present in few methanotrophs [28].

The advent of high-throughput sequencing technologies enables more comprehensive assessments of structural and functional traits of the soil microbiome [29]. Early studies in the Amazon Basin demonstrated the impacts of land-use change on soil microbiota [30–34]. Concerning methane-cycling, Meyer et al. [35] reported that forest-to-pasture conversion in the Amazon rainforest has a direct bearing on these microorganisms, with the strongest responses exhibited by methanotrophs, rather than methanogens. Moreover, recent works have shown that CH_4-cycling dynamics are altered due to shifts in the taxonomic community structure, with a significant increase in the abundance and activity of methanogens in pasture soils [13, 36, 37]. However, it remains untested how functional components of the community (i.e., functional gene content) relate to these changes, and what soil abiotic and biotic factors are driving the alterations on the CH_4 cycling communities following forest-to-pasture conversion.

Land-use change affects several soil properties, including organic matter, carbon and nutrient cycling, and pH, which are known to affect methanogenesis and methanotrophy [19, 21]. Land-use change also impacts soil structure and porosity [38], which negatively impacts O_2 diffusion affecting both methanogenesis and methanotrophy [39]. A better understanding of the abiotic and biological processes

regulating soil CH_4 flux will allow for predicting which conditions, including land-use and management practices, can achieve higher soil CH_4 oxidation rates and lower net CH_4 emissions [19, 40]. On the other hand, despite the importance of abiotic factors, biotic interactions (i.e., microbe-microbe interactions) are another driver of microbial diversity [41]. It has been suggested that the interaction network of methanotrophs and non-methanotrophs modulate methane oxidation [42, 43], while the methanogens are syntrophically related between and with syntrophic bacteria and cannot exist independently [44–46].

In this study, we seek to determine the relationship between CH_4-cycling and microbial metagenomic attributes along a forest-to-pasture conversion gradient in the Western Amazon Basin. We use metagenomic sequencing from field-collected soil samples to assess microbial gene content and high-resolution taxonomic structure and analyze the interaction networks of these microorganisms in forest and pasture soils. Lastly, we use a multimodel approach to determine the relationship between CH_4 fluxes (*in situ* measurements), changes in soil physicochemical properties, and the shift in microbial community traits. The study aimed to: 1) determine the community composition of methanogens and methanotrophs, and their relative abundance into the whole microbiota; 2) determine the interaction range, interaction strength, and keystoneness of CH_4-cycling microorganisms; 3) identify the shift in metabolic traits from methane-cycling communities in forest and pasture soils, and 4) identify the changes in soil abiotic factors underlying shifts in CH_4-cycling communities and its relation to CH_4 fluxes.

Methods

Study area and sampling

This study was carried out at “Agropecuaria Nova Vida” (09°54'58" S 63°02'27" W), a 20.000-ha cattle ranch in the central region of Rondônia state, Brazil (Fig. 1). Habitats in this area belong to the Amazon biome, where the local climate is humid tropical and classified as Af (Koppen’s classification), with a mean annual temperature of 25.5ºC and precipitation of 2200 mm [47]. The soil is classified as Ultisol [48]. Forest soil comprises areas of primary (undisturbed) forest. The pasture areas were established in 1972, following slash-and-burn soil preparation with no mechanical interventions or chemical fertilization [49]. Pastures are managed by cattle rotation, fire applied only to control eventual pests, mechanical removal of invasive trees, and at least one record of liming 15 years before the sampling.

Soil and gas samples were taken in April 2017 at the end of the rainy season, which occurs from October through May. The samples were collected from three sites in each land-use (forest and pasture). Within each site, a transect with five points 50-m distant was established (Fig. 1), totaling 15 sampling points (n = 15) per land-use. At each point, surface litter material was removed and static cylindrical chambers (with removable lid) were used for gas sampling. The dimensions of the chambers were 12 x 30 cm (total volume of 6.3 L) and were inserted 3 cm deep in the soil. Gas samples were taken four times after closed chambers (0, 10, 20, and 30 min), using plastic syringes and pre-evacuated (< 0.05 kPa) 20-mL glass vials as gas sample containers. The vials were crimp sealed with 20-mm blue butyl rubber stopper (Chemglass

Life Sciences, Vineland, NJ, USA). The measurements of gas concentration were made in the laboratory within one week, as detailed below.

After gas sampling, soil samples were collected from the top layer (0–10 cm) and kept on ice. Once in the laboratory, one part of the soil sample was kept at -20°C for DNA extraction, and the other part was kept at 4°C for the measurement of chemical properties. Additional undisturbed soil cores (5.0 x 5.0 cm) were collected in the center of the topsoil layer (0–10 cm) for soil physical analyses.

Methane flux measurement and processing

The CH_4 concentration in the gas samples was measured using an SRI8610C gas chromatograph (GC) (SRI Instruments Inc., USA), with a flame ionization detector (FID). Nitrogen was used as a carrier gas at a flow rate of 25 cm^3 min^{-1}. Oven and detector temperatures were 50 and 150°C, respectively. Standard CH_4 samples (White Martins, Rio de Janeiro, Brazil) were used for GC calibration. CH_4 flux calculations were performed using a simple linear regression model of change in the concentration as a function of the incubation time within the chamber. Daily CH_4 flux (F, μg CH_4-C m^{-2} h^{-1}) was calculated according to Eq. 1, proposed by Ussiri and Lal (2009):

$$F = \left(\frac{\Delta g}{\Delta t}\right)\left(\frac{\mathrm{V}}{\mathrm{A}}\right)k$$

1

Where $\Delta g/\Delta t$ is the linear change in CH_4 concentration inside the chamber (i.e., μg CH_4-C chamber min^{-1}), V is the chamber volume (m^3), A is the surface area circumscribed by the chamber (m^2) and k is the time conversion factor (60 min). Chamber CH_4 concentration was previously converted from molar mixing ratio (unit of parts per million, ppm), determined by GC analysis, to volumetric mass density by assuming ideal gas law.

Soil physical-chemical properties

Soil chemical properties were analyzed at the Laboratory of Soil Fertility, Luiz de Queiroz College of Agriculture, USP, Brazil, as described by [51]. Briefly, soil pH was measured from $CaCl_2$ suspension. Organic matter (OM) was measured by the colorimetric method. Total Nitrogen (TN) was extracted and determined by the combustion catalytic oxidation method. Available phosphorus (P) and potassium (K^+) were determined by colorimetry and atomic emission spectroscopy, respectively. Calcium (Ca) and magnesium (Mg) were determined by atomic absorption spectrometry, aluminum (Al) was determined by acid-base titration. The total exchangeable bases (EB) was calculated as the sum of Ca^{2+}, Mg^{2+}, and K^+. Potential acidity (H) is the sum of Al^{3+} and H^+. The potential cation exchange capacity ($CEC_{pH7.0}$) was calculated as the sum of EB and potential acidity. The percentage of base saturation (v) was calculated as the relation between EB and CEC. The aluminum saturation (m) was calculated as the relation of Al^{3+}

and effective cation exchange capacity (ECEC), where ECEC is the total amount of exchangeable cations plus Al^{3+}. Available micronutrients (Fe^{2+}, Mn^{2+}, Zn^{2+}, and Cu^{2+}) were extracted with diethylenetriaminepentaacetic acid (DTPA).

To determine macropores and micropores, soil cores were saturated and subjected to drainage at -6 kPa in the tensile table, as described in Teixeira et al. (2017). Soil macroporosity (Mac) comprised pores larger the 50 μm, which drained at -6 kPa. Microporosity (Mic) included pores smaller than 50 μm (micrometer) that retained water at -6 kPa. Soil bulk density (BD) was calculated with the relation of dry soil mass (oven-dried at 105 ºC for 24 h) and cylinder volume. Total porosity (TP) was calculated using two methods: (i) soil saturation (TPs), and (ii) calculated (TPc) with the relationship of BD and particle density (PD) measured with a pycnometer.

DNA extraction and quantitative PCR analyses

DNA extraction was carried out from 250 mg of each soil sample using PowerLyzer PowerSoil DNA Isolation Kit (Qiagen, Hilden, Germany), according to the manufacturer's protocol with modifications. Briefly, after adding C1 solution, the stirring and centrifugation times were extended to 15 min and 3 min respectively [53]. DNA quality and concentration were measured using a NanoDrop 1000 spectrophotometer (Thermo Scientific, Waltham, USA).

The abundance of methanogens and methanotrophs was assessed through qPCR assays targeting the marker genes *mcr*A, *pmo*A, and *mmo*X, using referenced primers set (Supplementary Table 1), which were purchased from Sigma-Aldrich Chemical (Sigma Aldrich, St. Louis, MO, USA). For each qPCR assay, standard curves were constructed based on purified PCR products, performed with DNA extracted from strains of *Methanolinea mesophila* (DSMZ 23604), used for *mcr*A gene, and *Methylosinus sporium* (DSMZ 17706) used to construct the *pmo*A and *mmo*X standard curves. Both strains were obtained from the German Collection of Microorganisms and Cell Cultures (DSMZ) (Leibniz Institut DSMZ, Braunschweig, Germany). The starting gene copy number was calculated with the DNA copy number calculator at the URI Genomics and Sequencing Center website (http://cels.uri.edu/gsc/cndna.html). The standard curves included six DNA concentrations in a range of 10^1–10^7 DNA copies μL^{-1}.

The qPCR reactions were made in 10 μL final volume, containing 5 μL of 2x SYBR Green ROX qPCR Master Mix (Thermo Scientific), 0.5 μM of each primer, 0.5 μM bovine serum albumin (BSA) (Thermo Scientific), 1μL of total DNA (10–30 ng/μl) and nuclease-free water. The qPCR amplifications were carried out as follows: 95°C for 30 s; 42 cycles of 94°C for 15 seg, 56 °C for 30 seg, 72°C for 30 seg. Also, a melting curve was included, between 65°C and 95°C with increments of 0.5°C at 5 seg. The reactions were carried out in a StepOne Plus thermocycler (Applied Biosystems, USA), and the results were analyzed using StepOne Software v2.3 (Applied Biosystems, USA). The R^2 values remained between 96% and 101% in all the trials, and the slope remained at -3.28 ± 0.15, -3.27 ± 0.10, and − 3.30 ± 0.14 in the *pmo*A, *mmo*X, and *mcr*A assays, respectively. Results were expressed as gene copy numbers per gram of soil (log copy number g^{-1} soil).

Whole metagenome shotgun sequencing and annotation

Three out of five sampling points per site were selected for whole metagenomic sequencing (WGS). In total, 18 DNA metagenome samples (nine from each land-use) were processed using the TruSeq kit (Illumina, San Diego, CA, USA) for library preparation, according to the manufacturer's protocol for WGS in an Illumina HiSeq 2500 platform (two×100 bp paired-end). The WGS sequences were pre-processed and annotated with the web application server Metagenomic Rapid Annotations using Subsystems Technology (MG-RAST), pipeline version 4 [54]. Briefly, the raw sequences were processed by quality control (QC) using SolexaQA software by removing low-quality segments using the "Dynamic Trim" method [55], according to the lowest Phred score of 15 and a maximum of 5 bases below the Phred score. Subsequently, the artificial replicate sequences and singletons were removed [56].

The protein-coding region (features) identification was based on the protein database M5nr for a non-redundant integration of many protein databases [57]. The taxonomic origins of the features were determined using the RefSeq database [58], and the functional profiles were analyzed according to the SEED subsystem. Annotation parameters were those recommended by Randle-Boggis et al. [59] using MG-RAST: maximum *e*-value cut-off of 1e-5, and minimum alignment length of 15 bp, while the minimal identity cut-off was 60 and 80% for taxonomical and functional profiling respectively, allowing a trade-off between sensitivity and accuracy. Abundance profiles were determined using the 'Representative Hit Classification' method. During the analysis, features annotated as eukaryotic and viral sequences were removed, and the dataset was normalized based on the negative binomial distribution approach, using the 'DESeq' method [60] implemented in the MG-RAST.

Microbial co-occurrence networks

The taxonomic profiling from each dataset was used to infer co-occurrence networks of interacting bacteria and archaea at the species level. We used the SparCC method from the package 'SpiecEasi' [61] implemented in R v. 3.6.3 [62] to build the correlation matrix. Several metrics were used to explore the topology and strength of the networks (i.e., number of nodes and edges, weighted degree, the diameter of the network, modularity, and the clustering coefficient). We explored several centrality metrics (i. e., betweenness centrality, harmonic centrality, and closeness centrality) [63] to infer the 'keystoneness' of each node, which is defined as the ability of a species to alter the abundance of other species and the structure of the community [64]. Keystone taxa are highly connected taxa (i.e., high network centrality) that individually or in a guild exert a considerable influence on microbiome structure and functioning, thus its alterations can have knock-on effects on ecosystem functions and services (Banerjee et al., 2018). We selected eigenvector centrality for the analysis because it takes into account both the number of connections of a given node and its relevance in terms of influence within the network [66]. The calculations and network visualizations were done with the software Gephi 0.9.2 [67].

Statistical analysis

Average values of CH_4 flux, as well as the abundance of marker genes (*pmo*A, *mmo*X, and *mcr*A) and the gene ratios, were compared between the two land-use groups using the two-tailed Student's t-test, with Welch's correction (CI.95%). Soil properties were compared using the Multiple t-test methods (*t*-test per row) with Hol-Sidak correction. Statistical analyses and graphs were performed using GraphPad Prism software v.8.0.1 (GraphPad Software Inc., CA, USA).

Differences in taxonomic and functional profiles between whole microbiomes from pasture and forest soils were tested using permutational multivariate analysis of variance (PERMANOVA) and visualized using non-metric multidimensional scaling (NMDS), both based on Bray-Curtis dissimilarity index. PERMANOVA and NMDS were performed using PAST software [68]. Furthermore, the differential abundances of the well-known methanogens [23] and methanotrophs [26] were quantified considering the whole microbial communities, for which the abundance profile (total) was normalized using centred log ratio (clr) transformation [69]. Likewise, we compared the abundance of the enzymes pMMO, sMMO, and MCR on the functional profiles from forest and pasture soils. Lastly, we measured the differential abundance of the genes encoding key enzymes involved in the three methanogenic pathways (i. e., acetoclastic, hydrogenotrophic, and methylotrophic), according to the MetaCyc pathway mapping (Superpathway of methanogenesis; PWY-6830) [70]. The differential features were detected by comparing the $\log_2$ fold change (LFC) between forest and pasture soil, using the Wald test as implemented in the DESeq method in the R package 'DESeq2' [71]. DESeq ensures a shrinkage estimation of dispersions and fold-changes for each feature, resulting in high-accuracy estimates. The p-values were adjusted according to the Benjamini-Hochberg FDR method to avoid the inflation of type-I error [72].

The relationship between gene abundance (log-transformed) and soil properties from pasture and forest sites was analyzed using redundancy analysis (RDA) following Box-Cox transformation of the explanatory variables (soil properties). A similar analysis was performed to infer the relationship between taxa abundance and soil properties. The Hellinger transformation was applied to the taxonomic table to generate the distance matrix suitable for RDA [73]. The selection of explanatory variables was performed by the forward-selection method which has correct levels of type-I error and power [74]. The RDAs were performed using the CANOCO 5 software [75].

We used a multi-model inference approach [76] to determine the contribution or importance of soil biotic (abundance of functional groups or genes) and abiotic (physicochemical properties) factors on the CH_4 emissions. Because we aimed to compare the suitability of different types of microbial data, we carried out to separate analyses based on: i) abundance of genes *mcr*A, *pmo*A, and *mmo*X as quantified by qPCR, and ii) abundance of key enzymes involved in the methanotrophy and methanogenesis pathways obtained from WGS analysis. The two analyses were performed using the same set of physicochemical properties. To avoid multicollinearity, a set of predictor variables was chosen in each analysis, based on their collinearity with other properties (assessed using both Pearson correlation and variance inflation factor or VIF). For each of the datasets (i.e., functional groups or genes), we first created a global model using linear mixed-effects models (lme) in the R package 'nlme' [77]. This global model included all the selected explanatory variables as fixed effects, as well as 'site' as a random effect. To validate the global

model in terms of homoscedasticity and normality, residuals were analyzed using graphical tools. Then, we compared models with different sets of predictors using the function 'dredge' in the R package 'MuMIn' [78]. This function generates a set of models with all possible combinations of predictors and ranks them by second-order Akaike Information Criterion (AICc) [76]. In addition, we calculated the relative importance of the different predictor variables, which is based on the AIC weight of the models in which the variable appears.

Results

Increase in soil CH_4 flux and CH_4-cycling microorganisms after forest-to-pasture transition

Methane fluxes were higher in pasture than forest soils ($t = 1.97$, $p < 0.05$) (Fig. 2a). As expected, forest soil acted as a CH_4 sink, with an average of -67.14 ± 34.40 μg m^2 h^{-1} (95% CI: -140.9 to 6.64). Pasture soils, on the other hand, exhibited net CH_4 emissions, with an average of 23.82 ± 30.63 μg m^2 h^{-1} (95% CI: -41.88 to 89.53), although CH_4 consumption was observed at some sampling points.

A high abundance of methanogens (*mcr*A gene) was observed in pasture soils ($t = 13.96$, $p < 0.001$) (Fig. 2b). Different abundance patterns were observed among the methanotrophs based on the quantification of the *pmo*A and *mmo*X genes. While *mmoX*-harboring methanotrophs were more abundant in forest soils ($t = 6.56$, $p < 0.001$), *pmo*A-harboring methanotrophs were more abundant in pasture soils ($t = 8.55$, $p < 0.001$) (Fig. 2b). In addition, the gene ratios *pmo*A/*mcr*A and *mmo*X/*mcr*A were both higher in forest soils (Fig. 2c), but the differences were more significant for *mmo*X/*mcr*A ($t = 7.39$, $p < 0.001$). Despite the observed imbalance in the abundance of methanogens and methanotrophs, the CH_4 flux was poorly explained by both *pmo*A/*mcr*A and *mmo*X/*mcr*A gene ratios (Fig. 2d).

Changes to the taxonomic composition of CH_4-cycling communities

The taxonomic profiling of the whole metagenomic data set (RefSeq) revealed significant differences (PERMANOVA; $F = 4.6$ $p < 0.001$) in community composition between forest and pasture soils (Supplementary Figure S1). When exploring well-known methanogenic and methanotrophic communities, it was found that methanotrophs had a higher relative abundance than methanogens. Yet, methanogens were more diverse in terms of community members (Fig. 3a). The methanogenic community was comprised of 26 archaeal taxa (at species-level), belonging to seven orders among which the most frequent were Methanosarcinales (28%), Methanococcales (24%), Methanobacteriales (20%), and Methanomicrobiales (16%). Comparing land uses, methanotrophic taxa were more abundant in forest soils than those observed in pastures, while methanogens were more abundant in pasture soils, except for three species of *Methanocaldococcus* (i.e., *M. jannaschii*; *M. fervens*; *M. sp.* FS406-22; *M. vulcanius*) (Fig. 3b).

“Keystoneness” of methane-cycling taxa within microbial co-occurrence networks

Co-occurrence networks constructed from the taxonomic profiles from forest and pasture soils (Supplementary Figure S2) revealed differences in the interaction patterns of microbial communities (Table 2). Although the number of nodes (connected taxa) was similar in both soils, the number of correlations (edges) in forest soils was twice as higher than in pasture soils, indicating that the microbiota in the undisturbed forest soils is highly interconnected, whereas this property is lost due to land-use change. Indeed, the microbial network from forest soils consisted of fewer modules, a higher number of nodes per module, and twice the average edges per node than the network from pasture soils (Table 2; Fig. 4a-b).

Table 2
Topological parameters of co-occurrence networks of bacterial and archaeal species in forest and pasture soils and the interaction patterns of methane-cycling taxa.

Network features & connectedness of CH_4-cycling	Forest	Pasture
Nodes	1472	1452
Methanogens	26	26
Methanotrophs	5	5
Edges	104734	47010
Network Diameter	12	10
Average degree	142.3	64.7
Weighted degree	124.3	56.2
Average path length	4.2	4.2
Modularity	0.61	0.68
Number of modules	10	8
Average clustering coefficient	0.72	0.64
Edges from methane-cycling ***	3588 (3.4%)	750 (1.6%)
Edges within methane-cycling *	178 (0.2%)	62 (0.1%)
Edges methanogens-methanotrophs	0	0
Edges from methanogens ***	2988 (2.9%)	485 (1.0%)
Edges from methanotrophs *	776 (0.7%)	264 (0.6%)
Edges within methanogens *	176 (0.2%)	58 (0.1%)
Edges within methanotrophs	2 (0.0%)	4 (0.0%)

Nodes represent microbial genera with at least a significant ($p<0.01$) and positive (SparCC > 0.75) correlations. Edges represent the number of connections/correlations obtained by SparCC analysis. Modularity represents the strength of connections between the nodes within different communities. The number of modules is the number of communities in the network. Network diameter indicates the longest distance between nodes in the network. Average path-length is the average length of the shortest path between any possible pairs of networks nodes. The average degree represents the average number of edges per node in the graph. Weighted degree is the sum of the weights of all edges attached to the node. The average clustering coefficient indicates how nodes are embedded in the network. Interactions of methane-cycling represent the percentage of edges connecting nodes from methanogens and methanotrophs, significant differences between land uses were tested by the “two-proportion Z-test” (* $p<0.05$; ** $p<0.01$; *** $p<0.001$).

Among the nodes from both networks, 31 belonged to methane-cycling taxa, including 26 methanogens and 5 methanotrophs (Fig. 4a-b). Methane-cycling taxa exhibited a greater degree of interactions within the microbial networks from forest soils, including interactions within methanogens but also between methanogens and methanotrophs and other microorganisms not directly related to CH_4 metabolism (Table 2). Overall, the average number of connections from methane-cycling taxa was three-fold higher in forests than in pasture soils. In addition to being more connected, they also showed a greater ecological relevance, exhibiting higher centrality within the microbial networks in forest soils (Fig. 4c-d).

Increase in methanogenesis markers and decrease in methanotrophy markers in pasture soils

Metagenomic functional profiles significantly differed ($F = 2.05$; $p = 0.05$) between forest and pasture soils, Supplementary Figure S3). Genes encoding the subunits of the pMMO enzyme were slightly more abundant in pasture soils, while the subunits of sMMO were more abundant in forest soils (Fig. 5). Concerning methanogenesis, we analyzed the genes encoding MCR, the terminal enzyme for all three methanogenesis pathways. The analysis revealed that the two isoforms of methyl coenzyme M reductase (MCR-I and MCR-II) were more abundant in pasture soils. MCR-I was fivefold more abundant in pasture than in forest soils (Wald test, $p < 0.001$), while MCR-II was onefold higher (Fig. 5).

All metabolic pathways of methanogenesis are increased in pasture soils

Acetoclastic methanogenesis was the most abundant pathway in both pasture and forest soils (Fig. 6). A total of 11 out of 12 genes were more abundant in pasture soils in comparison to forest soils. The gene encoding for the enzyme formylmethanofuran (formyl-MFR) dehydrogenase (EC 1.2.7.12), was more abundant in forest soils (Fig. 6). This enzyme catalyzes a reversible reaction in hydrogenotrophic methanogenesis by reducing carbon dioxide (CO_2) to form carboxy-MFR. However, the alternative forms of this enzyme, tungsten-containing- and molybdenum-containing formyl-MFR dehydrogenases, were more abundant in pasture soils. The analysis also found an increased abundance of methylotrophic methanogenesis in pasture soils, as observed in the higher abundance of all enzymes involved in this pathway (Fig. 6).

Changes in soil abiotic factors impact the abundance of methanogens and methanotrophs

Pasture soils showed higher pH and consequently a reduced percentage of Al saturation, as well as higher available micronutrients (Fe, Mn, Zn, and Cu). Other soil chemical properties showed no detectable differences between land uses (Supplementary Table 2). We observed changes in soil structure, specifically in the ratio of micro- and macropores, with a predominance of micropores in pasture soils and macropores in forest soils.

The RDA on the relationships between methane-cycling gene abundances and soil properties (Fig. 7a) revealed a clear effect of soil properties on the differentiation between land uses. Soil porosity, pH, and micronutrient content (i.e., Mn, Cu, and Zn) were the main drivers influencing gene abundance profiles. The abundance of CH_4-cycling taxa was similarly associated with soil properties, but included significant effects only from soil macroporosity and Cu content (Fig. 7b).

Metagenomic functional profile is a better predictor of CH_4 flux than qPCR quantification of marker genes

Only predictors of low multicollinearity were included in the multi-model inference analyses to prevent overparameterization. Therefore, based on the correlations among the several edaphic factors initially considered, only pH, OM, Cu, and the mac/mic ratio were included in further analysis (Supplementary Figure S4). Similarly, for gene abundance data we included only *mcr*A and the ratio *mmo*X/*pmo*A, while from the metagenomic dataset we selected the gene encoding the enzyme sMMO (methanotrophic) and four methanogenic enzymes (Supplementary Figure S5).

The multi-model inference including gene abundance data produced a total of 63 models. The ten best models, as ranked by AICc, included mostly edaphic properties and only 30% (3/10) included the gene ratio of methanotrophic genes (Fig. 8a). In fact, the four best models did not include any microbial gene data and the R^2 did not improve significantly when including them in the model. Overall, R^2 values were relatively low, with only 16–29% of the methane flux explained by the best models. The higher contribution of edaphic properties can also be seen in the importance of the predictors (Fig. 8a), which is calculated as the sum of 'Akaike weights' over all the models that include explanatory variables. The macropore/micropore ratio, Cu, and OM content were the most important drivers of CH_4 flux, followed by the gene ratio *mmo*X/*pmo*A (Fig. 8a).

Results were different when including metagenomic data instead of qPCR gene abundance. Of the 512 models produced by the analysis, the 10 models with the highest AICc included at least one methane-cycling enzyme, usually from methanogenesis pathways (Fig. 8b). Soil OM was the only edaphic factor included in the best models. Moreover, these models explained 38–75% of methane fluxes, with most models exhibiting an R^2 higher than 0.5. The enzyme methanol–corrinoid protein methyltransferase (EC 2.1.1.90), implicated in methylotrophic methanogenesis, was the most important factor predicting CH_4 fluxes. Other enzyme-encoding genes following in importance were those from hydrogenotrophic and acetoclastic methanogenesis (Fig. 6) and the enzyme sMMO from methanotrophy.

Discussion

The disruption of natural ecosystems associated with land-use change often leads to increased emissions of CH_4 to the atmosphere [17]. Our results support previous evidence showing that forest-to-

pasture conversion in the Amazon rainforest reverts the role of soil from sink to source of CH_4 [11–13, 80]. Recent studies have shown that this phenomenon is associated with alterations in community traits of soil methane-cycling microorganisms [13, 35, 37]. Our findings evidenced the direct effect of the land-use change on soil CH_4-cycling microbial communities, specifically characterized by shifts in the taxonomic and functional groups of methanotrophs and the increase in abundance of methanogens. We found that type II methanotrophs *Methylosinus trichosporium* and *Methylocella silvestris*, and the type I *Methylococcus capsulatus*, are amongst the most abundant taxa in Amazon forest soils, consistent with findings by Meyer et al. [35]. However, these authors also found an overall high abundance of *Methylocystis rosea* (type II), which was not observed in our analyses. Interestingly, both studies found a greater abundance of *Methylacidiphilum infernorum* in forest soils, an acidophilic methanotrophic aerobic bacterium from the phylum Verrucomicrobia. This bacterium grows optimally at pH ~ 2.5 [81], and thus could be well suited for the acidic conditions of Amazon soils. In concordance with Meyer et al. [35], we also found a great diversity of methanogenic archaea inhabiting both forest and pasture soils, which belonged to 7 out of the 8 well-known orders from the phylum Euryarchaeota [23]. Among the most abundant methanogens in pasture soils was the hydrogenotrophic Rice Cluster I, which is widely distributed and generally found living in rice roots [82]. Other abundant species were from the genera *Methanosarcina* and *Methanocella*, which seem to be ubiquitous in aerated soils and adapted to fluctuating oxic-anoxic conditions as soil water content changes [83].

The results of our network analyses suggested a loss of connectedness and influence of CH_4-cycling microbes within the soil microbiota following forest-to-pasture conversion. We hypothesize that changes in the interaction patterns of these microorganisms could be related to changes in nutrient availability. Nutrient availability can increase negative interactions between microbes by stimulating competition [41], thus affecting the stability of the microbial communities [84]. Here, nutrient availability in pasture soils may have been increased by tree removal, changes in soil cover and slash-and-burn management practices [49, 85]. Slash-and-burn often leads to an increase in soil nutrient availability due to the input of nutrient-rich ash [86, 87]. The nutrient input following slash-and-burn has been reported to shape bacterial community composition in Amazonian soils, dominated by fast-growing high nutrient requiring (i.e., copiotrophic) taxa (e.g., Actinobacteria) and fewer oligotrophic stress-tolerant taxa (e.g., Chlamydiae, Planctomycetes and Verrucomicrobia) in deforested soils [30, 88].

Microbial interaction networks may arise more complex in conditions limiting substrate availability since co-occurrence leads to greater metabolic exchange [89]. We assume that deforestation disrupts the microbial food web, in a way that CH_4-cycling microorganisms are less relevant. For instance, methanotrophs showed a significant reduction of connections between them and with other non-methane-cycling microbes in pasture soils (Fig. 4). Although not autotrophs, methanotrophs are base of food webs acting as an accessible carbon source for heterotrophs [90–92]. In this regard, a network meta-analysis conducted by Ho et al. [43] revealed a CH_4-derived food web in diverse ecosystems, in which methylotrophs were always present underlying the cross-feeding between methanotrophs and methylotrophs, whereas non-methanotrophic communities were site-specific and not consistent among

the diverse ecosystems. Interestingly, in that analysis, the clustering around methanotrophs was not confirmed in pasture soils, suggesting that other microorganisms compatible with methanotrophs and more complex metabolic routes exist in pasture soils [43].

Methanotrophs that carry the soluble form of the enzyme MMO (sMMO) were depleted by land-use change whereas those the harboring particulate form of this enzyme (pMMO) were enhanced (Figs. 2 and 5). These results constitute strong evidence of functional diversification of the methanotrophic community due to the forest-to-pasture conversion. The selective process of *pmo*A- and *mmo*X-type methanotrophs is likely a consequence of changes in soil physical and chemical properties imposing a niche differentiation for these microorganisms [43, 93]. For instance, γ-proteobacterial methanotrophs (mainly *pmo*A-type) are predominant in neutral pH soils, while α-proteobacterial methanotrophs, comprising mostly *mmo*X type, are well adapted to acidic soils [94]. Consistently, the methanotrophic species with the highest reduction in abundance in pasture soils was *Methylocella silvestris* (Beijerinckiaceae), a *mmo*X-type with moderate acidophilic preference [26] usually found in forest soils [95].

Methanogenesis pathways also differentiated along with the forest-to-pasture conversion, with increased hydrogenotrophic and methylotrophic methanogenesis in pasture soils (Fig. 6). Methylotrophic methanogens (mainly from orders Methanosarcinales and Methanomassiliicoccales) are major contributors to CH_4 biosynthesis in marine sediments, where other methanogens are outcompeted by sulphate-reducing bacteria [22]. Yet, recent studies have shown that methylotrophic methanogens are much more diverse and widespread than expected [24, 96, 97]. In this work, methylotrophic methanogens were mostly represented by *Methanosarcina* spp. [23, 98] and were most abundant in pasture soils, likely due to the higher availability of methylated compounds in these soils. Methyl-fermenting methanogens from the family Methanosarcinaceae possess a complete Wood–Ljungdahl pathway and can oxidize methyl groups to carbon dioxide at standard conditions of high pressure of H_2, whereas outcompete methyl-reducing methanogens [99, 100].

The observed microbial changes are likely to be linked to modifications in their abiotic environment. Land-use change induced modifications in soil abiotic factors, including pH, micronutrient content (i.e., Cu, Mn, Zn), and soil macro- and micro-pores (Supplementary Table 2), consistently with previous reports in the Amazon region [34, 101–103]. The increase in pH in pasture soils was positively associated with the abundance of methanogens and *pmo*A-type methanotrophs. Furthermore, the inversely proportional abundance of *pmo*A and *mmo*X methanotrophs also seemed to be associated by soil pH, since methanotrophs comprise taxons adapted to different pH (i.e., from alkaline to acidic soils) [19, 26, 94, 104]. Interestingly, higher Cu levels in pasture soils also appeared to be a key driver of the *mmo*X/*pmo*A ratio and the abundance of methanotrophs (Fig. 7). Experimental work has demonstrated that Cu content can alter the physiology of methanotrophs [105]. For instance, the expression of sMMO (*mmo*X) can be suppressed at high Cu conditions, while increased expression of *pmo*A has been observed at high Cu conditions, a phenomenon termed the “copper switch” [106, 107]. The ratio macropores/micropores was drastically reduced in pasture soils, mostly due to compaction induced by animal trampling [108], and it

consistently with shifts in the relative abundance of methanogens and methanotrophs (Fig. 7). The increased proportion of micropores over macropores in pasture soils could constitute an important factor driving niche differentiation of both methanogens (strict anaerobes) and methanotrophs (aerobes).

Besides characterizing changes in methane-cycling communities and their abiotic environment, we were also able to evaluate their capacity to predict methane emissions. The functional metagenomic profiling enabled a better prediction of CH_4 emissions than data derived from qPCR quantification, possibly given the higher resolution of metagenomic data to split functional markers into different pathways. We also detected a slight change in the predictive value of different edaphic factors to explain CH_4 flux when combined with either gene quantification data (qPCR) or metagenomic functional profile data (Fig. 8). For instance, soil porosity, followed by Cu and OM, were the most important predictors when qPCR data was used, while OM was the main abiotic predictor in models with functional metagenomic data. Such differences arise from the contrasting relationships between different biotic and abiotic variables (Fig. 7). For example, Cu was associated with qPCR and taxonomic data, but it did not outweigh them because enzymes were better predictors of CH_4 fluxes. Interestingly, OM, which was not related to qPCR or taxonomic data in RDA, became the abiotic variable with the largest importance. This result suggests that OM, which shows a slight increase in pasture soils ($+ \sim 8.75 g\ dm^{-3}$), is influencing CH_4 fluxes through a mechanism that is not directly associated to the microbial variables analyzed. A possible mechanism is via the link of methanogenesis to the availability of substrates resulting from the degradation of organic matter [109].

Conclusion

Overall, this study supports strong evidence that soil methane-cycling communities are affected by forest-to-pasture conversion, resulting in an increase of methanogens and the reduction of methanotrophs in pasture soils. Methylotrophic and hydrogenotrophic methanogenesis were the most increased methanogenic pathways in pasture soils, but acetoclastic was the most abundant pathway in our metagenomic data. Methane uptake potential was affected in pasture soil, with a reduction in sMMO-harboring methanotrophs. The observed shifts in methane-cycling communities with land-use change were associated with an increase in pH, soil compaction, and soil organic matter and micronutrient content in pasture soils. Moreover, land-use change seems to reduce interactions between methane-cycling and with the rest of the community. Future research should focus on the nature of the interactions of these microorganisms, specifically in the context of food webs, to better understand the dynamics of methane-cycling communities in the Amazon soils.

Declarations

Ethics approval and consent to participate

Not applicable

Consent for publication

Not applicable

Competing Interests

The authors declare that they have no competing interests

Availability of data and materials

The metagenome dataset resulting from our QC and feature annotation are publicly available in the MG-RAST database, project number mgp88746. Other data on soil properties and microbial analysis are available in the are included in this published article and its supplementary information files.

Funding

This research was supported by the São Paulo Research Foundation (FAPESP- 2014/50320-4; 2015/13546-7; 2016/24695-6; 2017/09643-2; 2017/18327-7; 2018/09117-1; 2018/05223-1; 2020/12890-4), National Science Foundation - Dimensions of Biodiversity (DEB 1442214), Coordination for the Improvement of Higher Education Personnel - Brasil (CAPES- 001; 88887.185941/2018-00) and National Council for Scientific and Technological Development (CNPq - 311008/2016-0; 140953/2017-5; 307670/2021-0). MT was supported by Food from Thought, a program funded by Canada First Research Excellence Fund (CFREF) and KD was supported by the Natural Sciences and Engineering Research Council (NSERC).

Author contributions

DOA, LFS and SMT designed the study with contributions from LWM and PBC. The supporting research project was conceived and coordinated by SMT, JLMR, PBC, and BJMB. Gas measurement and sample collection were performed by LFS, PBC, JLMR. LFS performed gas chromatography and analyzed gas data. DOA and LFS conducted the molecular analysis. DOA and LFS analyzed the metagenomic data. MTM analyzed soil properties. DOA conducted the statistical analyses with support of MT. DOA and LFS discussed the results with KM, AMV, and LWM. SMT funding. SMT and KD advised. DOA wrote the first draft with contributions from LFS, MT, and LWM. KD, KM, LWM, MT and JLM critically revisions. All the authors approved the final version of the manuscript.

Acknowledgments

We would like to thank the Large Scale Biosphere-Atmosphere Program (LBA), coordinated by the National Institute for Amazon Researches (INPA), for the use and availability of data, for logistical support and infrastructure during field activities. We thank the owners and staff of Agropecuária Nova Vida for logistical support; the owners Mr. Aristeu, Dr. Rigoberto and Mr. Tocandira for permitting access to its lands. We thank Wagner Picinini and Alexandre Pedrinho for their field soil sampling assistance.

Authors' information (Orcid ID)

Dasiel Obregón Alvarez https://orcid.org/0000-0002-5786-1114

Leandro Fonseca de Souza https://orcid.org/0000-0002-0774-7428

Lucas William Mendes https://orcid.org/0000-0003-0980-7006

Moacir Tuzin de Moraes https://orcid.org/0000-0001-9772-9137

Micaela Tosi https://orcid.org/0000-0001-6552-951X

Andressa Monteiro Venturini https://orcid.org/0000-0002-5901-1658

Kyle M. Meyer https://orcid.org/0000-0001-8846-7411

Plínio Barbosa de Camargo https://orcid.org/0000-0002-0696-3778

Brendan J.M. Bohannan https://orcid.org/0000-0003-2907-1016

Jorge L. Mazza Rodrigues https://orcid.org/0000-0002-6446-6462

Kari E. Dunfield https://orcid.org/0000-0003-1316-0452

Siu Mui Tsai https://orcid.org/0000-0002-3733-6312

References

[1] Strand J, Soares-Filho B, Costa MH, Oliveira U, Ribeiro SC, Pires GF, et al. Spatially explicit valuation of the Brazilian Amazon Forest's Ecosystem Services. Nat Sustain 2018;1:657–64. https://doi.org/10.1038/s41893-018-0175-0.

[2] Nepstad DC, Stickler CM, Soares-Filho B, Merry F. Interactions among Amazon land use, forests and climate: Prospects for a near-term forest tipping point. Philos Trans R Soc B Biol Sci 2008;363:1737–46. https://doi.org/10.1098/rstb.2007.0036.

[3] Aragão LEOC, Poulter B, Barlow JB, Anderson LO, Malhi Y, Saatchi S, et al. Environmental change and the carbon balance of Amazonian forests. Biol Rev 2014;89:913–31. https://doi.org/10.1111/brv.12088.

[4] Pereira EJ de AL, de Santana Ribeiro LC, da Silva Freitas LF, de Barros Pereira HB. Brazilian policy and agribusiness damage the Amazon rainforest. Land Use Policy 2020;92:104491. https://doi.org/10.1016/j.landusepol.2020.104491.

[5] Artaxo P. Working together for Amazonia. Science (80-) 2019;363:323. https://doi.org/10.1126/science.aaw6986.

[6] Rajão BR, Soares-filho B, Nunes F, Börner J, Machado L, Assis D, et al. The rotten apples of Brazil's agribusiness 2020:0–3.

[7] Barona E, Ramankutty N, Hyman G, Coomes OT. The role of pasture and soybean in deforestation of the Brazilian Amazon. Environ Res Lett 2010;5:024002. https://doi.org/10.1088/1748-9326/5/2/024002.

[8] Malhi Y, Roberts JT, Betts RA, Killeen TJ, Li W, Nobre CA. Climate change, deforestation, and the fate of the Amazon. Science (80-) 2008;319:169–72. https://doi.org/10.1126/science.1146961.

[9] Lapola DM, Martinelli LA, Peres CA, Ometto JPHB, Ferreira ME, Nobre CA, et al. Pervasive transition of the Brazilian land-use system. Nat Clim Chang 2014;4:27–35. https://doi.org/10.1038/nclimate2056.

[10] Reay D, Smith P, van Amstel A. Methane and climate change. Earthscan; 2010.

[11] Steudler P a., Melillo JM, Feigl BJ, Neill C, Piccolo MC, Cerri CC. Consequence of forest-to-pasture conversion on CH 4 fluxes in the Brazilian Amazon Basin. J Geophys Res 1996;101:18547–54. https://doi.org/10.1029/96JD01551.

[12] Fernandes SAP, Bernoux M, Cerri CC, Feigl BJ, Piccolo MC. Seasonal variation of soil chemical properties and CO 2 and CH 4 fluxes in unfertilized and P-fertilized pastures in an Ultisol of the Brazilian Amazon. Geoderma 2002;107:227–41.

[13] Meyer KM, Morris AH, Webster K, Klein AM, Kroeger ME, Meredith LK, et al. Belowground changes to community structure alter methane-cycling dynamics in Amazonia. Environ Int 2020;145. https://doi.org/10.1016/j.envint.2020.106131.

[14] Kotsyurbenko OR, Chin KJ, Glagolev M V., Stubner S, Simankova M V., Nozhevnikova AN, et al. Acetoclastic and hydrogenotrophic methane production and methanogenic populations in an acidic West-Siberian peat bog. Environ Microbiol 2004;6:1159–73. https://doi.org/10.1111/j.1462-2920.2004.00634.x.

[15] Conrad R. The global methane cycle: Recent advances in understanding the microbial processes involved. Environ Microbiol Rep 2009;1:285–92. https://doi.org/10.1111/j.1758-2229.2009.00038.x.

[16] Aronson EL, Allison SD, Helliker BR. Environmental impacts on the diversity of methane-cycling microbes and their resultant function. Front Microbiol 2013;4:1–15. https://doi.org/10.3389/fmicb.2013.00225.

[17] McDaniel MD, Saha D, Dumont MG, Hernández M, Adams MA. The effect of land-use change on soil CH4 and N2O fluxes: a global meta-analysis. Ecosystems 2019;22:1424–43. https://doi.org/10.1007/s10021-019-00347-z.

[18] Nazaries L, Murrell JC, Millard P, Baggs L, Singh BK. Methane, microbes and models: Fundamental understanding of the soil methane cycle for future predictions. Environ Microbiol 2013;15:2395–417. https://doi.org/10.1111/1462-2920.12149.

[19] Tate KR. Soil methane oxidation and land-use change - from process to mitigation. Soil Biol Biochem 2015;80:260–72. https://doi.org/10.1016/j.soilbio.2014.10.010.

[20] Malyan SK, Bhatia A, Kumar A, Kumar D, Singh R, Kumar SS, et al. Methane production , oxidation and mitigation: A mechanistic understanding and comprehensive evaluation of in fluencing factors. Sci Total Environ 2016;572:874–96. https://doi.org/10.1016/j.scitotenv.2016.07.182.

[21] Serrano-Silva N, Sarria-Guzmán Y, Dendooven L, Luna-Guido M. Methanogenesis and Methanotrophy in Soil: A Review. Pedosphere 2014;24:291–307. https://doi.org/10.1016/S1002-0160(14)60016-3.

[22] Conrad R. Importance of hydrogenotrophic, aceticlastic and methylotrophic methanogenesis for methane production in terrestrial, aquatic and other anoxic environments: A mini review. Pedosphere 2020;30:25–39. https://doi.org/10.1016/S1002-0160(18)60052-9.

[23] Evans PN, Boyd JA, Leu AO, Woodcroft BJ, Parks DH, Hugenholtz P, et al. An evolving view of methane metabolism in the Archaea. Nat Rev Microbiol 2019;17:219–32. https://doi.org/10.1038/s41579-018-0136-7.

[24] Söllinger A, Urich T. Methylotrophic methanogens everywhere - physiology and ecology of novel players in global methane cycling. Biochem Soc Trans 2019;47:1895–907. https://doi.org/10.1042/BST20180565.

[25] Rospert S, Linder D, Ellermann J, Thauer RK. Two genetically distinct methyl-coenzyme M reductases in Methanobacterium thermoautotrophicum strain Marburg and ΔH. Eur J Biochem 1990;194:871–7. https://doi.org/10.1111/j.1432-1033.1990.tb19481.x.

[26] Knief C. Diversity and habitat preferences of cultivated and uncultivated aerobic methanotrophic bacteria evaluated based on pmoA as molecular marker. Front Microbiol 2015;6. https://doi.org/10.3389/fmicb.2015.01346.

[27] McDonald IR, Bodrossy L, Chen Y, Murrell JC. Molecular ecology techniques for the study of aerobic methanotrophs. Appl Environ Microbiol 2008;74:1305–15. https://doi.org/10.1128/AEM.02233-07.

[28] Banerjee R, Jones JC, Lipscomb JD. Soluble Methane Monooxygenase. Annu Rev Biochem 2019;88:409–31. https://doi.org/10.1146/annurev-biochem-013118-111529.

[29] Fierer N. Embracing the unknown: disentangling the complexities of the soil microbiome. Nat Rev Microbiol 2017;15:579–90. https://doi.org/10.1038/nrmicro.2017.87.

[30] Rodrigues JLM, Pellizari VH, Mueller R, Baek K, Jesus EDC, Paula FS, et al. Conversion of the Amazon rainforest to agriculture results in biotic homogenization of soil bacterial communities. Proc Natl Acad Sci U S A 2013;110:988–93. https://doi.org/10.1073/pnas.1220608110.

[31] Mendes LW, de Lima Brossi MJ, Kuramae EE, Tsai SM. Land-use system shapes soil bacterial communities in Southeastern Amazon region. Appl Soil Ecol 2015;95:151–60. https://doi.org/http://dx.doi.org/10.1016/j.apsoil.2015.06.005.

[32] Navarrete AA, Taketani RG, Mendes LW, Cannavan F de S, Moreira FM de S, Tsai SM. Land-use systems affect Archaeal community structure and functional diversity in western Amazon soils. Rev Bras Ciência Do Solo 2011. https://doi.org/10.1590/S0100-06832011000500007.

[33] de Carvalho TS, da Conceição Jesus E, Barlow J, Gardner TA, Soares IC, Tiedje JM, et al. Land use intensification in the humid tropics increased both alpha and beta diversity of soil bacteria. Ecology 2016;97:2760–71. https://doi.org/10.1002/ecy.1513.

[34] Paula FS, Rodrigues JLM, Zhou J, Wu L, Mueller RC, Mirza BS, et al. Land use change alters functional gene diversity, composition and abundance in Amazon forest soil microbial communities. Mol Ecol 2014;23:2988–99. https://doi.org/10.1111/mec.12786.

[35] Meyer KM, Klein AM, Rodrigues JLM, Nüsslein K, Tringe SG, Mirza BS, et al. Conversion of Amazon rainforest to agriculture alters community traits of methane-cycling organisms. Mol Ecol 2017;26:1547–56. https://doi.org/10.1111/mec.14011.

[36] Venturini AM, Dias NMS, Gontijo JB, Yoshiura CA, Paula FS, Meyer KM, et al. Increased soil moisture intensifies the impacts of forest-to-pasture conversion on methane emissions and methane-cycling communities in the Eastern Amazon. Environ Res 2022;212:113139. https://doi.org/10.1016/j.envres.2022.113139.

[37] Kroeger ME, Meredith LK, Meyer KM, Webster KD, de Camargo PB, de Souza LF, et al. Rainforest-to-pasture conversion stimulates soil methanogenesis across the Brazilian Amazon. ISME J 2020. https://doi.org/10.1038/s41396-020-00804-x.

[38] Oguike PC, Mbagwu JSC. Variations in some physical properties and organic matter content of soils of coastal plain sand under different land use types. World J Agric Sci 2009;5:63–9.

[39] Fiedler S, Vepraskas MJ, Richardson JL. Soil redox potential: importance, field measurements, and observations. Adv Agron 2007;94:1–54. https://doi.org/10.1016/S0065-2113(06)94001-2.

[40] Fonseca De Souza L, Obregon Alvarez D, Domeignoz-Horta LA, Gomes FV, De Souza Almeida C, Merloti LF, et al. Maintaining grass coverage increases methane uptake in Amazonian pasture soils. BioRxiv 2021:2021.04.26.441496.

[41] Ratzke C, Barrere J, Gore J. Strength of species interactions determines biodiversity and stability in microbial communities. Nat Ecol Evol 2020;4:376–83. https://doi.org/10.1038/s41559-020-1099-4.

[42] Ho A, Mendes LW, Lee HJ, Kaupper T, Mo Y, Poehlein A, et al. Response of a methane-driven interaction network to stressor intensification. FEMS Microbiol Ecol 2020;96. https://doi.org/10.1093/femsec/fiaa180.

[43] Ho A, Angel R, Veraart AJ, Daebeler A, Jia Z, Kim SY, et al. Biotic interactions in microbial communities as modulators of biogeochemical processes: methanotrophy as a model system. Front Microbiol 2016;7:1–11. https://doi.org/10.3389/fmicb.2016.01285.

[44] Kotsyurbenko OR. Trophic interactions in the methanogenic microbial community of low-temperature terrestrial ecosystems. FEMS Microbiol Ecol 2005;53:3–13. https://doi.org/10.1016/j.femsec.2004.12.009.

[45] Fowler SJ, Toth CRA, Gieg LM. Community structure in methanogenic enrichments provides insight into syntrophic interactions in hydrocarbon-impacted environments. Front Microbiol 2016;7:1–13. https://doi.org/10.3389/fmicb.2016.00562.

[46] Zhang CJ, Pan J, Liu Y, Duan CH, Li M. Genomic and transcriptomic insights into methanogenesis potential of novel methanogens from mangrove sediments. Microbiome 2020;8:1–12. https://doi.org/10.1186/s40168-020-00876-z.

[47] Alvares CA, Stape JL, Sentelhas PC, de Moraes Gonçalves JL, Sparovek G. Köppen's climate classification map for Brazil. Meteorol Zeitschrift 2013;22:711–28. https://doi.org/10.1127/0941-2948/2013/0507.

[48] Embrapa. Empresa Brasileira De Pesquisa Agropecuaria-Embrapa Solos. Sistema brasileiro de classificação de solos. 5a edição,. Rio de Janeiro, Brazil: Embrapa soils; 2018.

[49] Feigl B, Cerri C, Piccolo M, Noronha N, Augusti K, Melillo J, et al. Biological survey of a low-productivity pasture in Rondônia state, Brazil. Outlook Agric 2006;35:199–208. https://doi.org/10.5367/000000006778536738.

[50] Ussiri DAN, Lal R. Long-term tillage effects on soil carbon storage and carbon dioxide emissions in continuous corn cropping system from an alfisol in Ohio. Soil Tillage Res 2009;104:39–47. https://doi.org/10.1016/j.still.2008.11.008.

[51] van Raij B, Andrade JC, Cantarella H, Quaggio JA. Análise química para avaliação da fertilidade de solos tropicais. Campinas: Instituto Agronômico de Campinas; 2001.

[52] Teixeira PC, Donagemma GK, Fontana A, Teixeira WG. Manual de métodos de análise de solo. vol. Reporte de. 3ª. Brasilia, DF: Embrapa; 2017.

[53] Venturini AM, Nakamura FM, Gontijo JB, da França AG, Yoshiura CA, Mandro JA, et al. Robust DNA protocols for tropical soils. Heliyon 2020;6. https://doi.org/10.1016/j.heliyon.2020.e03830.

[54] Meyer F, Paarmann D, Souza MD, Olson R, Glass EM, Kubal M, et al. The metagenomics RAST server – a public resource for the automatic phylogenetic and functional analysis of metagenomes. BMC Bioinformatics 2008;9:1–8. https://doi.org/10.1186/1471-2105-9-386.

[55] Cox MP, Peterson DA, Biggs PJ. SolexaQA: At-a-glance quality assessment of Illumina second-generation sequencing data. BMC Bioinformatics 2010;11:1–6.

[56] Gomez-Alvarez V, Teal TK, Schmidt TM. Systematic artifacts in metagenomes from complex microbial communities. ISME J 2009;3:1314–7. https://doi.org/10.1038/ismej.2009.72.

[57] Wilke A, Harrison T, Wilkening J, Field D, Glass EM, Kyrpides N, et al. The M5nr: a novel non-redundant database containing protein sequences and annotations from multiple sources and associated tools. BMC Bioinformatics 2012;13:2–5. https://doi.org/www.biomedcentral.com/1471-2105/13/141.

[58] O'Leary NA, Wright MW, Brister JR, Ciufo S, Haddad D, Mcveigh R, et al. Reference sequence (RefSeq) database at NCBI: current status, taxonomic expansion, and functional annotation. Nucleic Acids Res 2016;44:733–45. https://doi.org/10.1093/nar/gkv1189.

[59] Randle-boggis RJ, Helgason T, Sapp M, Ashton PD. Evaluating techniques for metagenome annotation using simulated sequence data. FEMS Microbiol Ecol 2016;92:1–15. https://doi.org/10.1093/femsec/fiw095.

[60] Anders S, Huber W. Differential expression analysis for sequence count data. Genome Biol 2010;11:1–12. https://doi.org/genomebiology.com/2010/11/10/R106.

[61] Friedman J, Alm EJ. Inferring Correlation Networks from Genomic Survey Data. PLoS Comput Biol 2012;8:1–11. https://doi.org/10.1371/journal.pcbi.1002687.

[62] R Core Team. R: A language and environment for statistical computing. 2021.

[63] Newman MEJ. The mathematics of networks. New Palgrave Encycl Econ 2008;2:1–12. https://doi.org/10.1093/acprof:oso/9780199206650.003.0006.

[64] Cagua EF, Wootton KL, Stouffer DB. Keystoneness, centrality, and the structural controllability of ecological networks. J Ecol 2019;107:1779–90. https://doi.org/10.1111/1365-2745.13147.

[65] Banerjee S, Schlaeppi K, van der Heijden MGA. Keystone taxa as drivers of microbiome structure and functioning. Nat Rev Microbiol 2018;16:567–76. https://doi.org/10.1038/s41579-018-0024-1.

[66] Ruhnau B. Eigenvector-centrality — a node-centrality? Soc Networks 2000;22:357–65.

[67] Bastian M, Jacomy M. Gephi: An Open Source Software for Exploring and Manipulating Networks Gephi : An Open Source Software for Exploring and Manipulating Networks. Proc. third Int. Conf. weblogs Soc. media, ICWSM 2009, San Jose, California, USA, May 17-20, 2009, 2009, p. 4–6. https://doi.org/10.13140/2.1.1341.1520.

[68] Hammer Ø, Harper D, Ryan P. PAST: paleontological statistics software package for education and data analysis. Palaeontol Electron 2001;4:9.

[69] Aitchison J. The Statistical Analysis of Compositional Data. GBR: Chapman & Hall, Ltd.; 1986.

[70] Caspi R, Billington R, Fulcher CA, Keseler IM, Kothari A, Krummenacker M, et al. The MetaCyc database of metabolic pathways and enzymes. Nucleic Acids Res 2018;46:D633–9. https://doi.org/10.1093/nar/gkx935.

[71] Love MI, Huber W, Anders S. Moderated estimation of fold change and dispersion for RNA-seq data with DESeq2. Genome Biol 2014;15:550. https://doi.org/10.1186/s13059-014-0550-8.

[72] Benjamini Y, Hochberg Y. Controlling the false discovery rate: a practical and powerful approach to multiple testing. J R Stat Soc Ser B 1995;57:289–300.

[73] Legendre P, Gallagher ED. Ecologically meaningful transformations for ordination of species data. Oecologia 2001;129:271–80. https://doi.org/10.1007/s004420100716.

[74] Legendre P, Oksanen J, ter Braak CJF. Testing the significance of canonical axes in redundancy analysis. Methods Ecol Evol 2011;2:269–77. https://doi.org/10.1111/j.2041-210X.2010.00078.x.

[75] ter Braak C, Šmilauer P. Canoco reference manual and user's guide: software of ordination (version 5.0). Microcomputer Power (Ithaca, NY. USA) 2012.

[76] Burnham KP, Anderson DR. Model selection and multimodel inference. Ed., 2nd. New York: Springer-Verlag Inc; 2002. https://doi.org/10.1007/b97636.

[77] Pinheiro J, Bates D. nlme: linear and nonlinear mixed effects models 2019.

[78] Barton K. MuMIn: Multi-Model Inference 2019.

[79] Kanehisa M, Goto S. KEGG : Kyoto encyclopedia of genes and genomes. Nucleic Acids Res 2000;28:27–30.

[80] Verchot L V., Davidson EA, Cattânio JH, Ackerman IL. Land-use change and biogeochemical controls of methane fluxes in soils of eastern Amazonia. Ecosystems 2000;3:41–56. https://doi.org/10.1007/s100210000009.

[81] Dunfield PF, Yuryev A, Senin P, Smirnova A V., Stott MB, Hou S, et al. Methane oxidation by an extremely acidophilic bacterium of the phylum Verrucomicrobia. Nature 2007;450:879–82.

https://doi.org/10.1038/nature06411.

[82] Conrad R, Erkel C, Liesack W. Rice Cluster I methanogens, an important group of Archaea producing greenhouse gas in soil. Curr Opin Biotechnol 2006;17:262–7. https://doi.org/10.1016/j.copbio.2006.04.002.

[83] Angel R, Claus P, Conrad R. Methanogenic archaea are globally ubiquitous in aerated soils and become active under wet anoxic conditions. ISME J 2012;6:847–62. https://doi.org/10.1038/ismej.2011.141.

[84] Lozupone CA, Stombaugh JI, Gordon JI, Jansson JK, Knight R. Diversity, stability and resilience of the human gut microbiota. Nature 2012;489:220–30. https://doi.org/10.1038/nature11550.

[85] Petersen IA, Meyer KM, Bohannan BJ. Consistent bacterial responses to land use change across the tropics. Front Ecol Evol 2019;7:600924. https://doi.org/10.1101/600924.

[86] De Souza Braz AM, Fernandes AR, Alleoni LRF. Soil attributes after the conversion from forest to pasture in Amazon. L Degrad Dev 2013;24:33–8. https://doi.org/10.1002/ldr.1100.

[87] Fujisaka S, Bell W, Thomas N, Hurtado L, Crawford E. Slash-and-burn agriculture, conversion to pasture, and deforestation in two Brazilian Amazon colonies. Agric Ecosyst Environ 1996;59:115–30. https://doi.org/10.1016/0167-8809(96)01015-8.

[88] Navarrete AA, Tsai SM, Mendes LW, Faust K, De Hollander M, Cassman NA, et al. Soil microbiome responses to the short-term effects of Amazonian deforestation. Mol Ecol 2015;24:2433–48. https://doi.org/10.1111/mec.13172.

[89] Zelezniak A, Andrejev S, Ponomarova O, Mende DR, Bork P, Patil KR. Metabolic dependencies drive species cooccurrence in diverse microbial communities. Proc Natl Acad Sci U S A 2015;112:E7156. https://doi.org/10.1073/pnas.1522642113.

[90] Hutchens E, Radajewski S, Dumont MG, McDonald IR, Murrell JC. Analysis of methanotrophic bacteria in Movile Cave by stable isotope probing. Environ Microbiol 2004;6:111–20. https://doi.org/10.1046/j.1462-2920.2003.00543.x.

[91] Kalyuzhnaya MG, Yang S, Rozova ON, Smalley NE, Clubb J, Lamb A, et al. Highly efficient methane biocatalysis revealed in a methanotrophic bacterium. Nat Commun 2013;4:1–7. https://doi.org/10.1038/ncomms3785.

[92] Karwautz C, Kus G, Stöckl M, Neu TR, Lueders T. Microbial megacities fueled by methane oxidation in a mineral spring cave. ISME J 2018;12:87–100. https://doi.org/10.1038/ismej.2017.146.

[93] Ho A, Lüke C, Reim A, Frenzel P. Selective stimulation in a natural community of methane oxidizing bacteria: Effects of copper on pmoA transcription and activity. Soil Biol Biochem 2013;65:211–6.

https://doi.org/10.1016/j.soilbio.2013.05.027.

[94] Kolb S. The quest for atmospheric methane oxidizers in forest soils. Environ Microbiol Rep 2009;1:336–46. https://doi.org/10.1111/j.1758-2229.2009.00047.x.

[95] Dunfield PF, Khmelenina VN, Suzina NE, Trotsenko YA, Dedysh SN. *Methylocella silvestris* sp. nov., a novel methonotroph isolated from an acidic forest cambisol. Int J Syst Evol Microbiol 2003;53:1231–9. https://doi.org/10.1099/ijs.0.02481-0.

[96] Borrel G, O'Toole PW, Harris HMB, Peyret P, Brugère JF, Gribaldo S. Phylogenomic data support a seventh order of methylotrophic methanogens and provide insights into the evolution of methanogenesis. Genome Biol Evol 2013;5:1769–80. https://doi.org/10.1093/gbe/evt128.

[97] Vanwonterghem I, Evans PN, Parks DH, Jensen PD, Woodcroft BJ, Hugenholtz P, et al. Methylotrophic methanogenesis discovered in the archaeal phylum Verstraetearchaeota. Nat Microbiol 2016;1:16170. https://doi.org/10.1038/nmicrobiol.2016.170.

[98] Buan NR. Methanogens: pushing the boundaries of biology. Emerg Top Life Sci 2018;2:629–46. https://doi.org/10.1042/etls20180031.

[99] Thauer RK, Kaster AK, Seedorf H, Buckel W, Hedderich R. Methanogenic archaea: Ecologically relevant differences in energy conservation. Nat Rev Microbiol 2008;6:579–91. https://doi.org/10.1038/nrmicro1931.

[100] Feldewert C, Lang K, Brune A. The hydrogen threshold of obligately methyl-reducing methanogens. FEMS Microbiol Lett 2020;367:1–7. https://doi.org/10.1093/femsle/fnaa137.

[101] Navarrete AA, Cannavan FS, Taketani RG, Tsai SM. A molecular survey of the diversity of microbial communities in different Amazonian agricultural model systems. Diversity 2010;2:787–809. https://doi.org/10.3390/d2050787.

[102] Navarrete AA, Soares T, Rossetto R, van Veen JA, Tsai SM, Kuramae EE. Verrucomicrobial community structure and abundance as indicators for changes in chemical factors linked to soil fertility. Antonie Van Leeuwenhoek Int J Gen Mol Microbiol 2015;108:741–52. https://doi.org/10.1007/s10482-015-0530-3.

[103] Ranjan K, Paula FS, Mueller RC, Jesus E da C, Cenciani K, Bohannan BJM, et al. Forest-to-pasture conversion increases the diversity of the phylum Verrucomicrobia in Amazon rainforest soils. Front Microbiol 2015;6:1–9. https://doi.org/10.3389/fmicb.2015.00779.

[104] Ghashghavi M, Jetten MSM, Lüke C. Survey of methanotrophic diversity in various ecosystems by degenerate methane monooxygenase gene primers. AMB Express 2017;7:162. https://doi.org/10.1186/s13568-017-0466-2.

[105] Semrau JD, Dispirito AA, Yoon S. Methanotrophs and copper. FEMS Microbiol Rev 2010;34:496–531. https://doi.org/10.1111/j.1574-6976.2010.00212.x.

[106] DiSpirito AA, Semrau JD, Murrell JC, Gallagher WH, Dennison C, Vuilleumier S. Methanobactin and the link between copper and bacterial methane oxidation. Microbiol Mol Biol Rev 2016;80:387–409. https://doi.org/10.1128/MMBR.00058-15.

[107] Murreil JC, Gilbert B, McDonald IR. Molecular biology and regulation of methane monooxygenase. Arch Microbiol 2000;173:325–32. https://doi.org/10.1007/s002030000158.

[108] Valladares GS, Batistella M, Pereira MG. Alterações ocorridas pelo manejo em latossolo, rondônia, amazônia brasileira. Bragantia 2011;70:631–7. https://doi.org/10.1590/s0006-87052011000300019.

[109] Conrad R, Klose M, Noll M. Functional and structural response of the methanogenic microbial community in rice field soil to temperature change. Environ Microbiol 2009;11:1844–53. https://doi.org/10.1111/j.1462-2920.2009.01909.x.

Figures

Figure 1

Geographical location of the study area. (**a)** Map of South America showing the Amazon Basin (green). The red dot indicates the location of the “Agropecuaria Nova Vida” Ranch wherein the study was conducted, situated in the Brazilian state of Rondônia. (**b)** Aerial view of the sampled sites. Codes

indicate the sampling transects (250 m) in primary forests (Forest 1,2,3), and pasture (Pasture 1,2,3) soils.

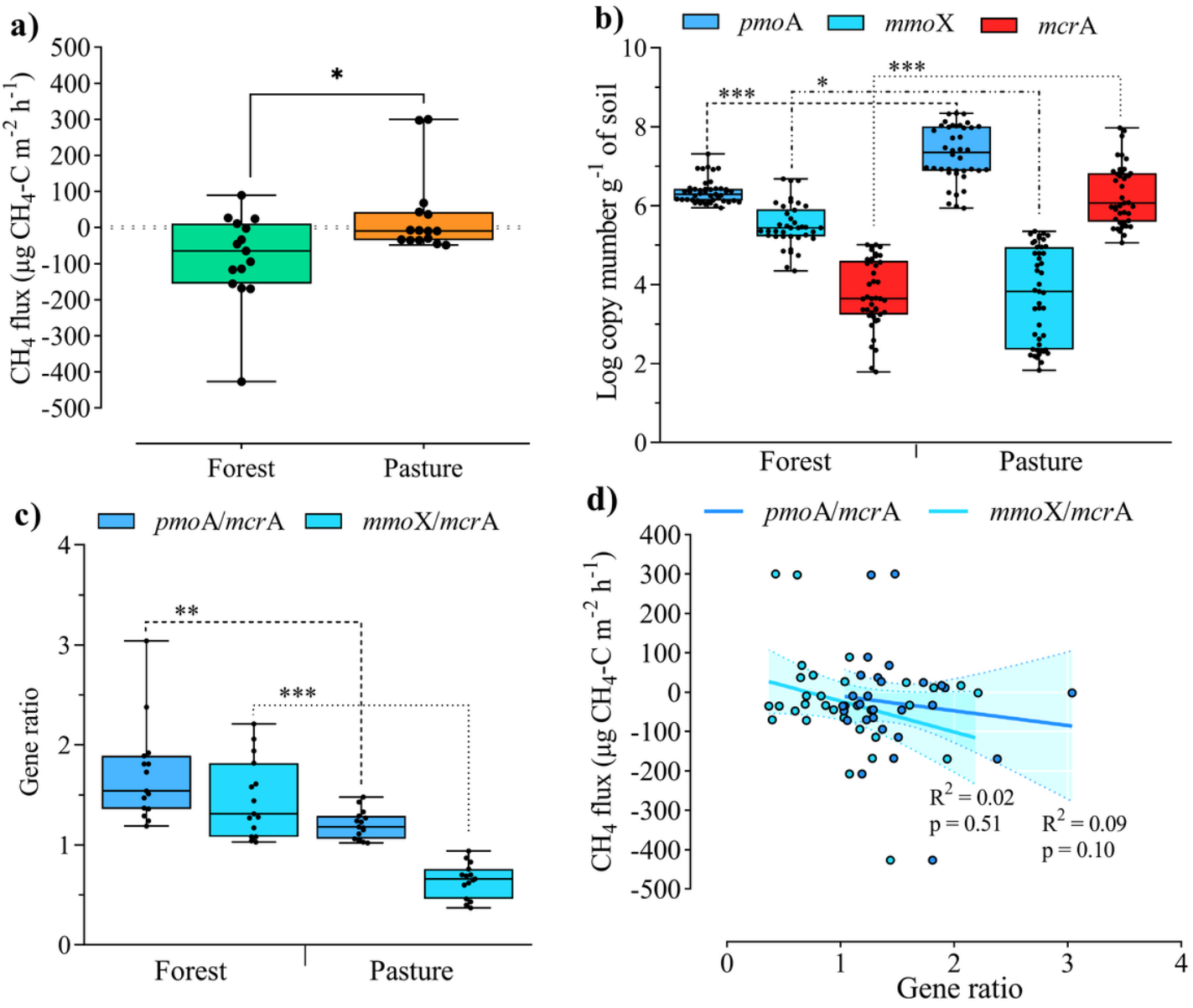

Figure 2

Methane flux and abundance of microbial functional genes associated with methanotrophy and methanogenesis in pasture and forest soils. (**a**) Box plot on methane flux in forest and pasture soils. (**b**) Abundance (gene copy number from DNA) of *mcr*A (methanogens) and *pmo*A and *mmo*X genes (methanotrophs). (**c**) Gene ratio indicating how many times the abundance of the functional genes of methanotrophy (*pmo*A and *mmo*X) contains the abundance of *mcr*A. Asterisks denote statistically significant differences (* $p<0.05$; ** $p<0.01$; *** $p<0.001$). (**d**) Relationships between the CH_4 flux and gene ratios, linear models were fitted for each ratio of genes, considering the two methanotrophic markers.

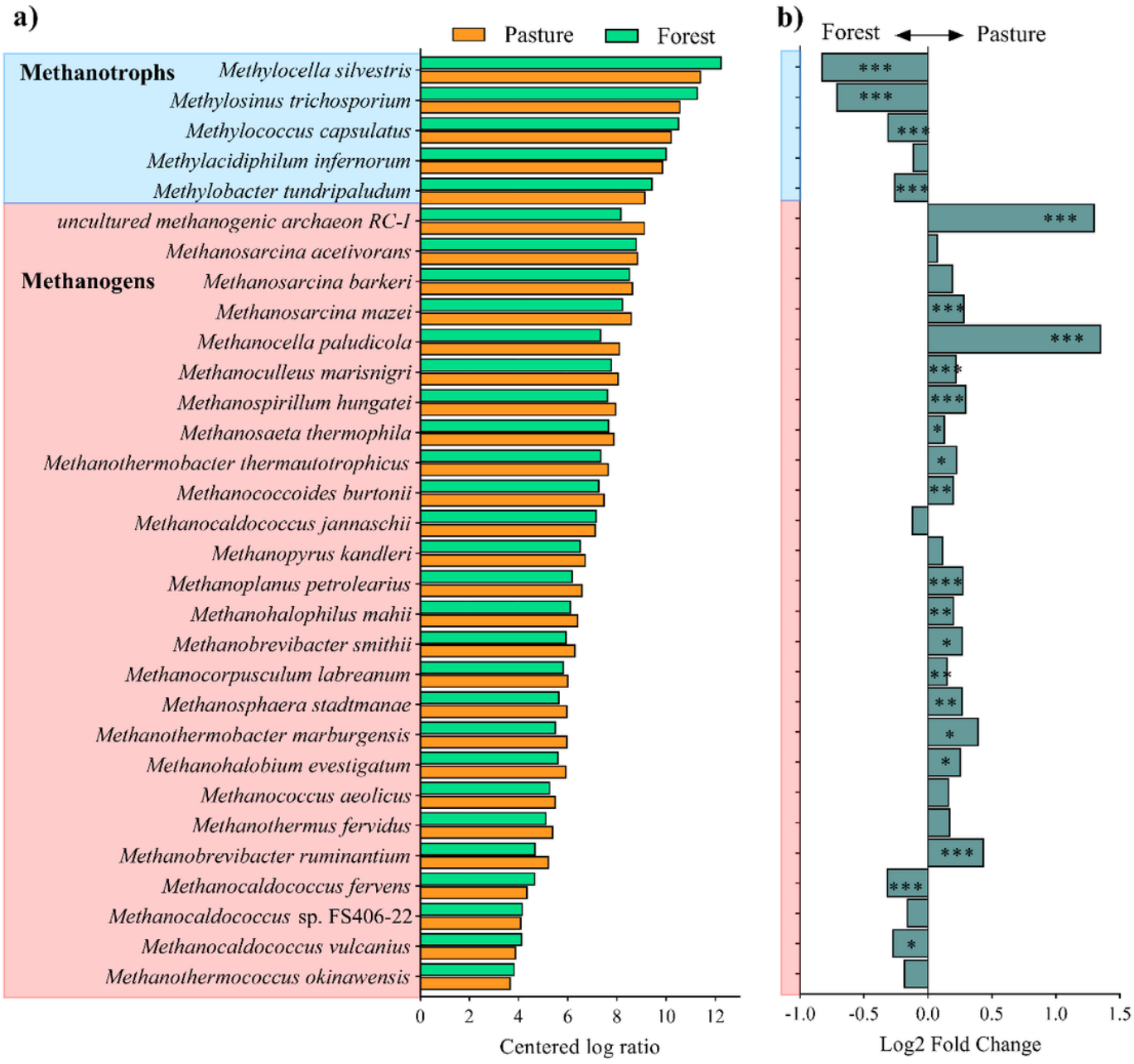

Figure 3

Changes to the relative abundance of methane-cycling taxa between forest and pasture soils. **(a)** Identity and relative abundance (centred log-ratio) of methanogenic archaea and methanotrophic bacteria (species level). **(b)** Differential abundance of each taxon between forest and pasture soils as $\log_2$ fold change (a value of 1 indicates that it is twice as abundant). Asterisks denote statistically significant differences according to Benjamini–Hochberg adjusted p-value (*** p<0.001, ** p<0.01, * p<0.05).

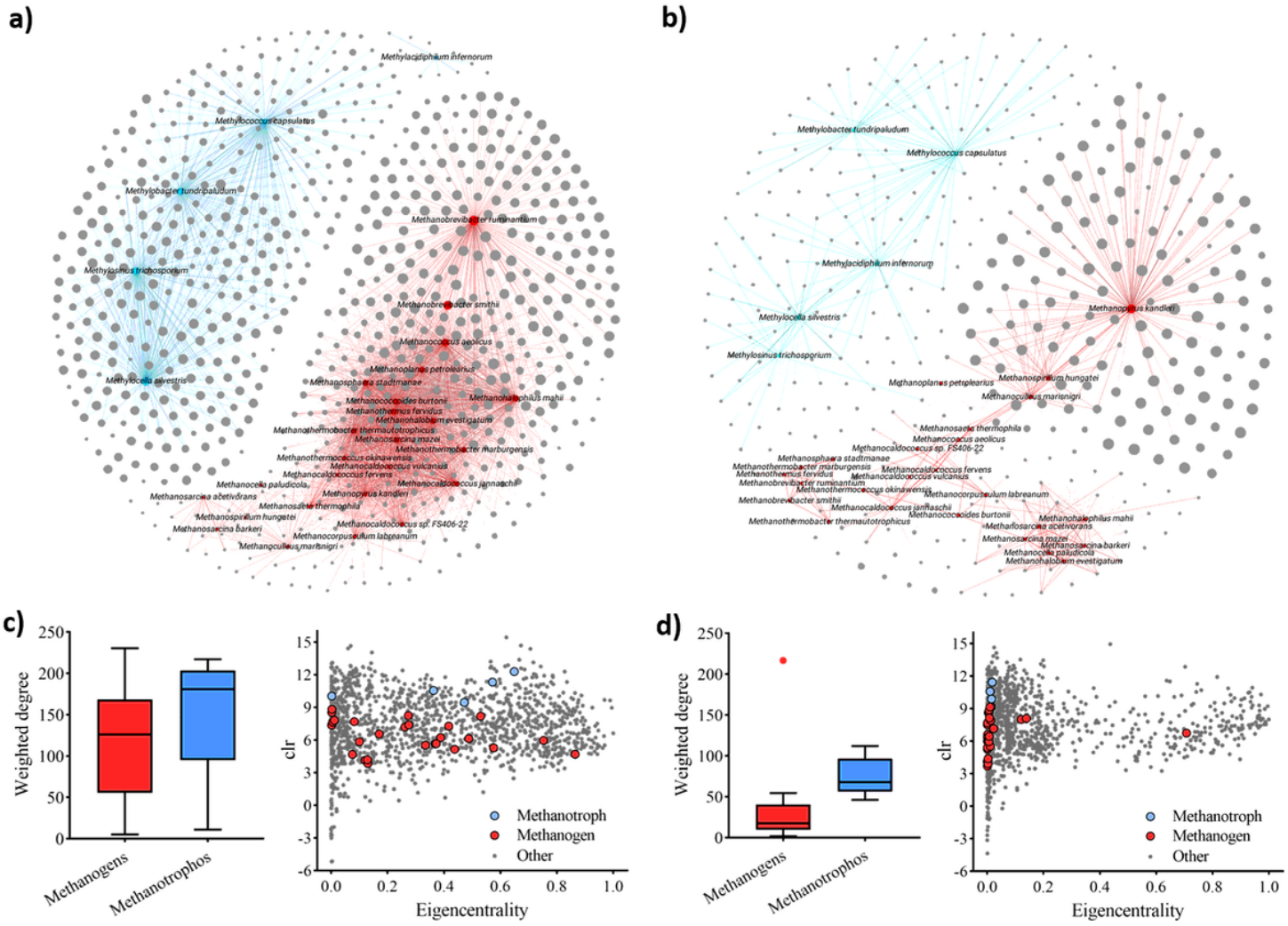

Figure 4

Co-occurrence networks of CH_4-cycling within the archaeal and bacterial communities from forest and pasture soils. The plots in (**a)** and (**b)** present partial networks, including the interactions of the methane-cycling taxa (species level) in forest and pasture soils respectively. In each plot, the nodes correspond to methanogens (red) and methanotrophs (blue), as well as all other taxa (gray) with which they co-occur. Connecting edges indicate significant ($p < 0.01$) and strong positive SparCC correlations ($r > 0.75$). Only nodes with at least one significant correlation are represented. The color of edges corresponds to its node of origin, and the size of the nodes is proportional to their eigencentrality value, which indicates the influence of a node in a network [63]. Bottom figures depict the 'keystoneness' of methane-cycling taxa within microbial interaction networks from (**c)** forest and (**d)** pasture soils, as its relationship with relative abundance (clr). Keystoneness was inferred in terms of connectedness (weighted degree) and eigencentrality in the networks.

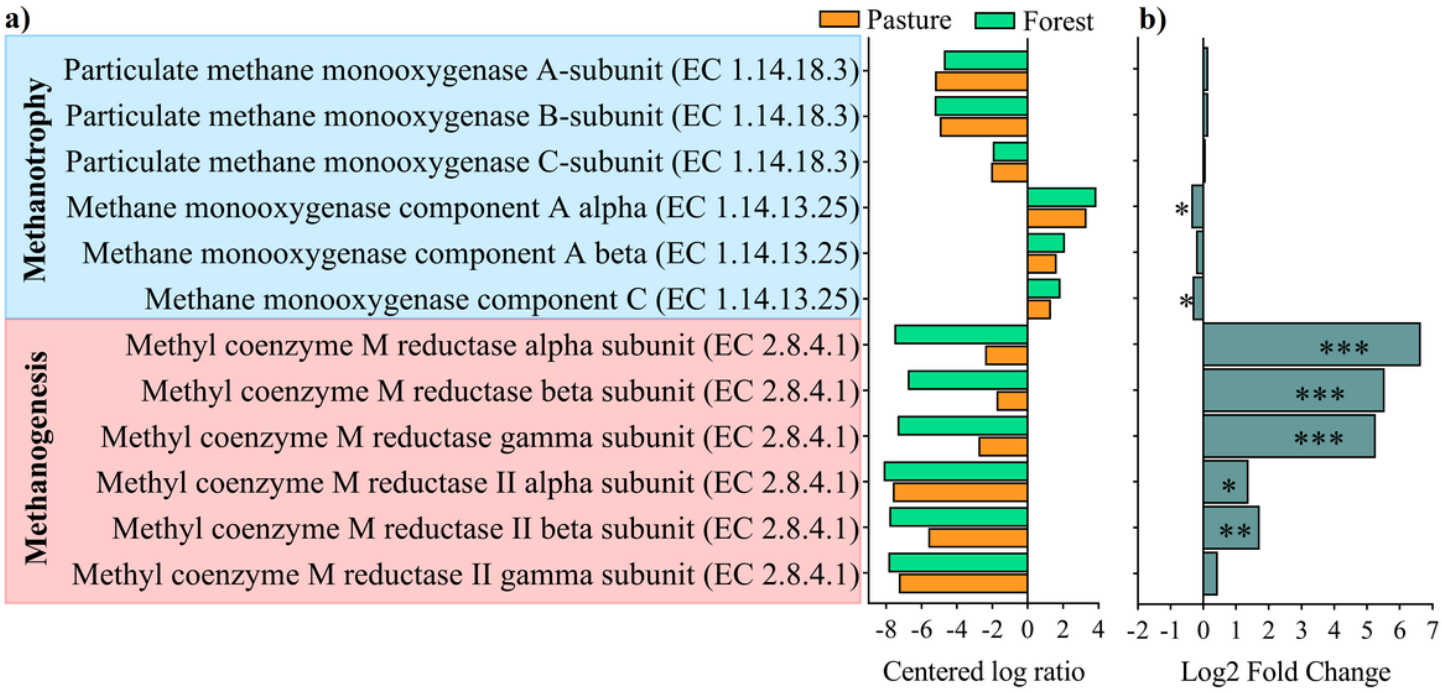

Figure 5

Differential abundance of the key enzymes of methanotrophy (MMO) and methanogenesis (MCR) between forest and pasture soils. **(a)** The two types of MMO are shown: the copper-containing membrane-bound enzyme particulate MMO (pMMO), and the cytosolic iron-containing soluble form (sMMO). The two forms of MCR are presented: MCR-I, which is present in all methanogens, and MCR-II, which is present in only a few methanogenic taxa. The relative abundance (clr) of main subunit is presented in each case. **(b)** Differential abundance of each enzyme (subunit) between forest and pasture soils as $\log_2$ fold change (a value of 1 indicates that it is twice as abundant). Asterisks denote statistically significant differences according to Benjamini–Hochberg adjusted p-value (*** $p<0.001$, ** $p<0.01$, * $p<0.05$).

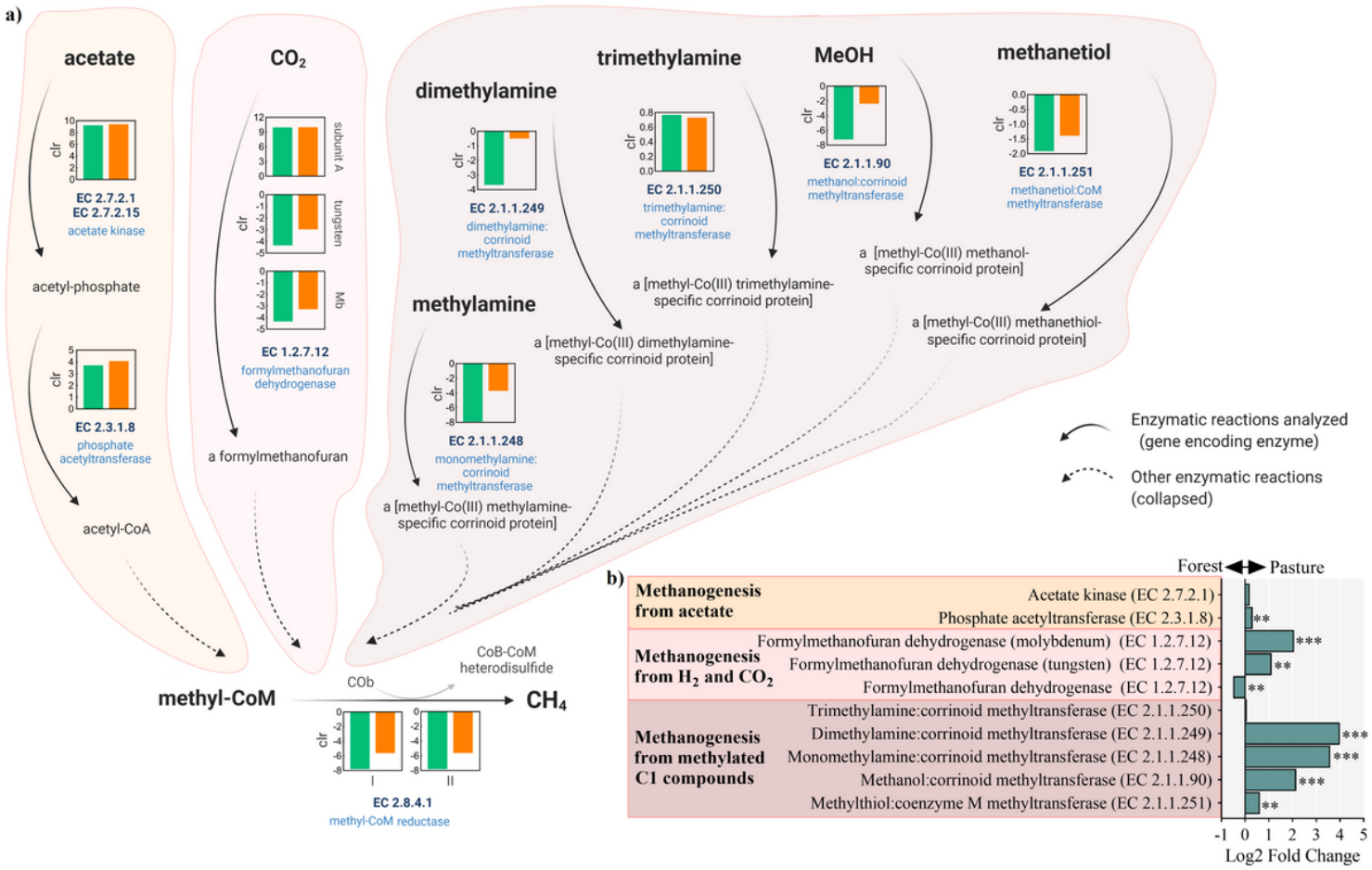

Figure 6

Differential abundance of the methanogenesis pathways from different substrates. **(a)** The abundance of the genes encoding enzymes from the first enzymatic reactions in each pathway are shown as their relative abundance (centered log-ratio, clr) in forest and pasture soils. The pathway maps are adapted from the “susperpathway of methanogenesis” according to the MetaCyc database [70]. Enzyme Commission (EC) numbers are provided according to MetaCyc and KEGG [79] database. **(b)** Differential abundance of the selected enzyme-encoding genes compared between forest and pasture soils, represented as the magnitude of $\log_2$ fold change. Asterisks denote statistically significant changes according to Benjamini–Hochberg adjusted p-value (*** p<0.001, ** p<0.01, * p<0.05).

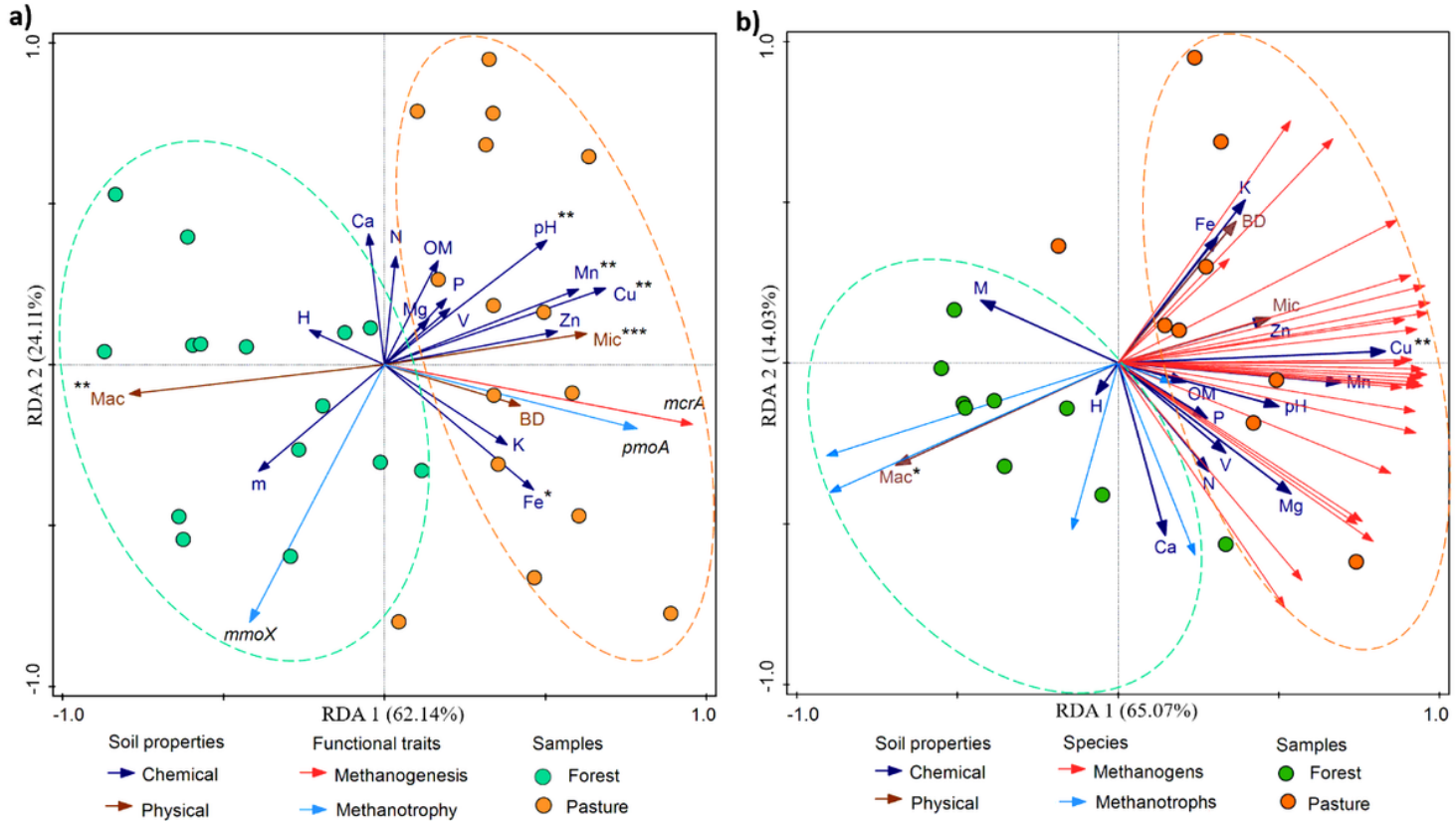

Figure 7

Redundancy analysis (RDA) linking soil physical and chemical properties with methane-cycling communities. **(a)** Analysis based on methane-cycling gene abundance profiles (*mcr*A, *pmo*A and *mmo*X) from qPCR quantification. **(b)** Analysis based on the composition of methanogenic and methanotrophic communities as obtained by metagenomic sequencing (at the species level). Vector points toward of increase for a given soil property and gene abundance, and its length indicates the strength of between-variable correlation and regarding the ordination scores. Asterisks indicate explanatory variables with significant contributions (* p <0.05, ** p <0.01, *** p <0.001).

a)

Model	*mmo X/pmo A*	*mcr A*	mac/mic	Cu	OM	pH	R^2	AICc	Δ AICc	Wi
1			-58.3		36.2		0.28	376.9	0	0.11
2			-59.5				0.20	377.2	0.29	0.09
3				58.2			0.19	377.6	0.62	0.08
4			-38.0	34.5			0.24	378.3	1.36	0.06
5	-27.4		-44.1				0.23	378.8	1.83	0.04
6	-52.2						0.16	379.0	2.01	0.04
7			-58.6			20.2	0.23	379.0	2.07	0.04
8				51.3	22.0		0.22	379.3	2.35	0.03
9			-46.1	19.9	30.4		0.29	379.3	2.40	0.03
10	-13.3		-51.0		32.2		0.28	379.6	2.65	0.03

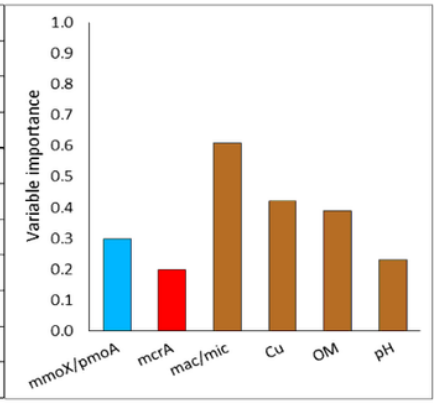

b)

Model	sMMO	EC: 2.1.1.90	EC: 1.2.7.12 (Mb)	EC: 2.7.2.1	EC: 2.1.1.248+9	OM	Mac/Mic	pH	Cu	R^2	AICc	Δ AICc	Wi
1		145.4	61.5	-53.9		62.1				0.68	227.3	0	0.07
2		87.4								0.38	227.4	0.20	0.06
3		102.3		-50.3		55.5				0.59	227.5	0.24	0.06
4		88.3				43.7				0.48	227.8	0.56	0.05
5		126.9	56.3			48.9				0.56	228.6	1.38	0.03
6	-95.7	161.3	106.8		87.4	61.8				0.75	228.6	1.39	0.03
7	-53.8	124.5				50.5				0.55	228.9	1.61	0.03
8	-60.0	171.5	62.4			57.0				0.65	228.9	1.65	0.03
9		120.1	47.8							0.44	229.0	1.70	0.03
10		97.2		-36.2						0.44	229.0	1.71	0.03

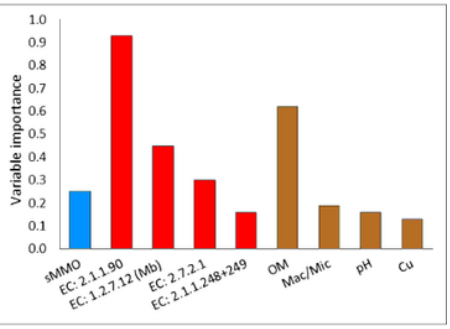

Figure 8

Best-fitting regression models explaining CH_4 flux in Amazonian soils along forest-to-pasture conversion. **(a)** Analysis based on the abundance of functional genes (qPCR). **(b)** Analysis based on the abundance of key functional enzymes assessed through metagenomics. In the tables, each row represents a model and each column is a different predictor variable (blue: functional markers of methanotrophy; red: functional markers of methanogenesis; brown: soil edaphic factors). Gray cells indicate variables that were not included in a particular model. For each analysis, the 10 best-fitting models (AICc) are presented. R^2: likelihood-ratio based pseudo-R-squared; ΔAICc: difference between the AICc of each model and the best model; Wi: Akaike weights.

Supplementary Files

This is a list of supplementary files associated with this preprint. Click to download.

- Supplementarymaterial.MetagenomeCH4Amazonsubmission.docx